Research of Pattern Formation, edited by R. Takaki, pp. 111–119.

Morphology and Formation Mechanism of Snow Polycrystals

Y. FURUKAWA

Institute of Low Temperature Science, Hokkaido University, Sapporo 060, Japan

Abstract. Morphological characters of a variety of snow polycrystals are summarized and the 70° concentrations of the c-axes angle between each component of a snow polycrystal are emphasized. The formation mechanisms of them are discussed on the basis of both the grain boundary structure expected from the Coinsidence-Site Lattice (CSL) concept and the formation of a cubic ice embryo during the ice nucleation process in the supercooled water droplet.

1. Introduction

Beautiful pictures of snow crystals as shown in the cover page of this book mislead us to believe that each of the snow crystals innumerably falling in the air possesses such a perfect hexagonal symmetry developed in two dimensions. But most of the natural snow crystals are actually polycrystals of twin type. The shapes of snow polycrystals include the twin prism (Fig. 1a), twelve-branched crystal (see cover photo), plane assemblage of the spatial type (spatial dendrite, Fig. 1b), plane assemblage of the radiating type (radiating dendrites, Fig. 1c), combination of bullets (Fig. 1d), crossed-plates crystal (Fig. 1e) and peculiar-shaped crystal (Fig. 1f). For these snow polycrystals, excepting the twelve-branched crystal whose branches develop in a plane, each component of the crystal extends in three dimensions. The morphology and the formation mechanism of these snow polycrystals, however, were given but of a scant attention because the difficulty of observation for the three-dimensionally developed crystals was not to be compared with that for single snow crystals.

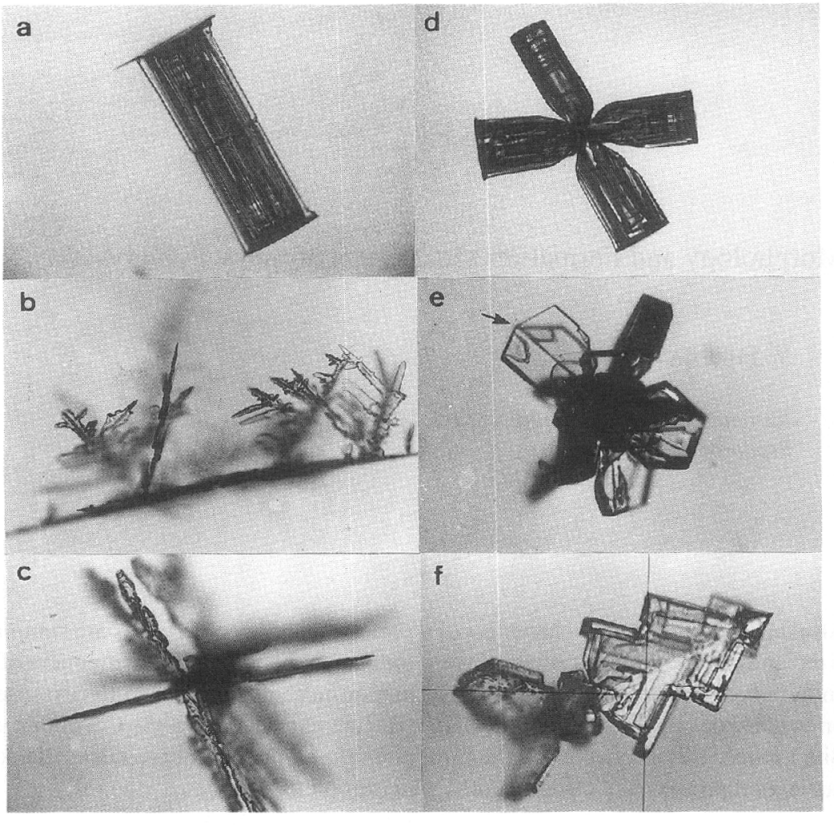

Fig. 1. A variety of snow polycrystals: (a) twin prisms, provided by Prof. Kawaguchi, National Institute of Polar Research; (b) spatial dendrite; (c) radiating dendrite; (d) combination of bullets, provided by Prof. Kawaguchi; (e) crossed-plates crystal (artificial); (f) peculiar-shaped crystal.

Observations of natural snow polycrystals have been carried out to clarify their structures for the last twenty years. Lee (1972) found that the frequency distribution of the c-axes angles of each component of snow polycrystal has a single high peak at 70° and that the a-axes of components coincide with each other. Uyeda and Kikuchi (1976a) and Kobayashi *et al.* (1976b) also conducted the same measurements and obtained the same results as Lee's. Figure 2 shows the frequency histograms of measured misorientations for several types of snow polycrystals. 70° peaks clearly appear for both the spatial dendrites and the radiating dendrites which are most popular types in snow polycrystals. In case of the combination of bullets, several other peaks are observed in addition to 70° peak. See the paper of Kobayashi and Furukawa (1975) for twelve-branched crystals.

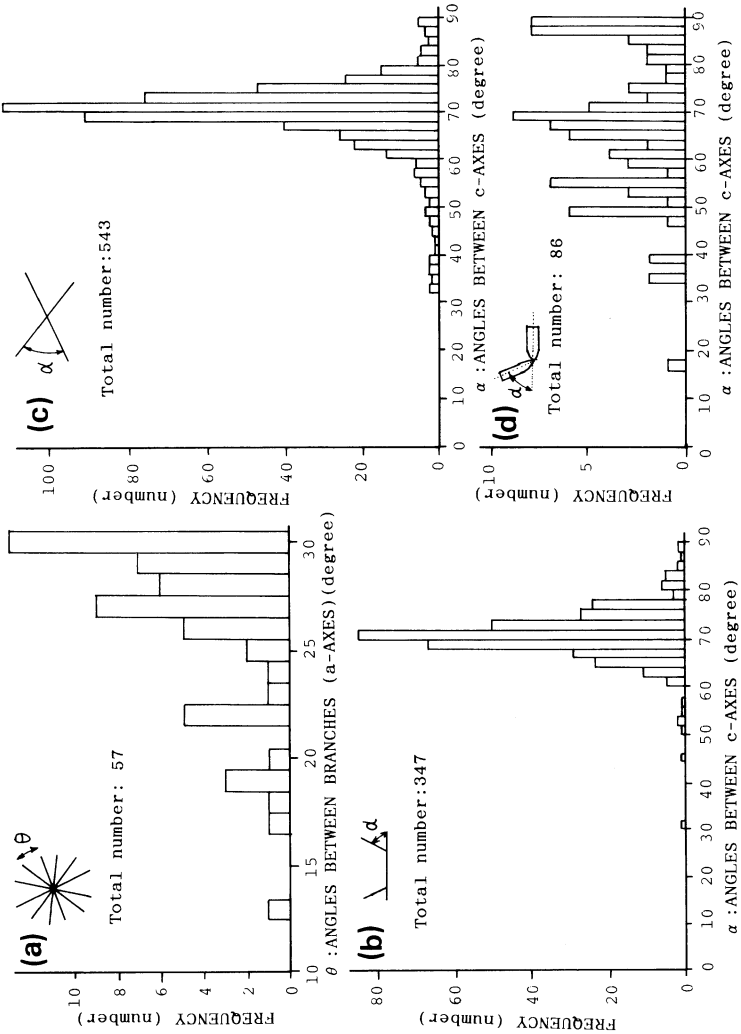

Fig. 2. Frequency distributions of measured misorientations: (a) twelve-branched dendrites, (b) spatial dendrites, (c) radiating dendrites, (d) combination of bullets.

The purpose of this review is to explain why the measured c-axes angles concentrate at 70° for almost all kinds of snow polycrystals.

2. Coincidence-Site Lattice (CSL) Boundaries in Ice Polycrystals

A grain boundary between any two crystals will take up such a position that the crystals exhibit more or less optimum matching. It has been made clear by many experimental evidences, as reviewed by Pumphley (1976), that boundary properties vary both with the misorientation and boundary plane, and that there are some specific misorientations at which boundaries behave as through they had lower energies than those with random misorientations.

It is known that for a certain misorientation about a rotational axis, there exists a three dimensional super-lattice on which lies a fraction ($1/\Sigma$, where Σ is a reciprocal density of coincidence-sites) of the lattice points in two crystal lattices.

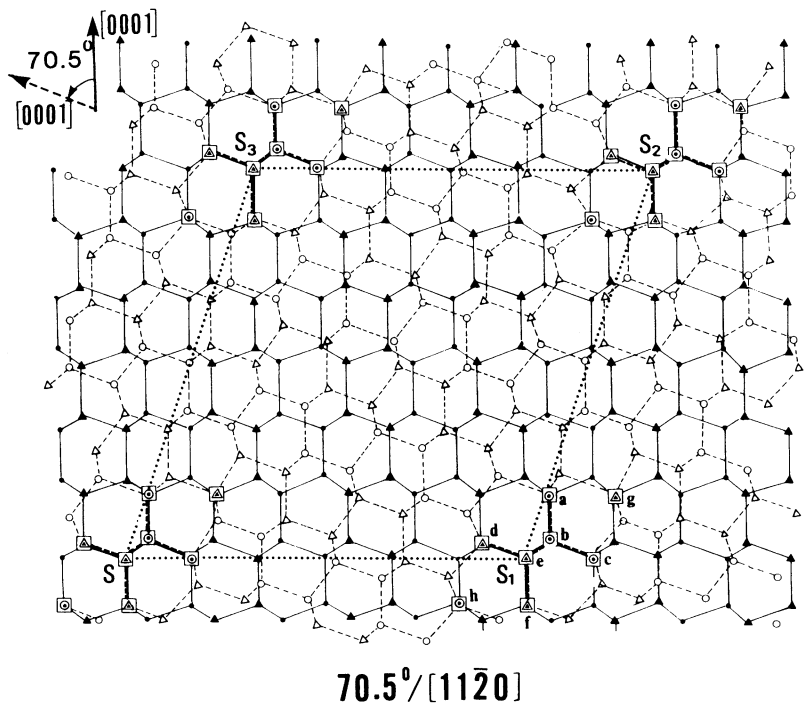

Fig. 3. Illustration of the interpenetrating crystal lattices after the rotation in a relation of 70.5°/[11$\bar{2}$0]. Solid and broken lines represent the hydrogen bonds before and after the rotation, respectively: projected along [11$\bar{2}$0].

This is referred to as a Coincidence-Site Lattice (CSL), whereby it has been suggested that a plane connecting lattice points of the CSL (namely, a plane of CSL conjugation) is a grain boundary showing a good atomic fitting. The best fitting and hence lowest energy may occur when the boundary follows a plane containing a higher density of coinsidence-sites.

Generally, a three dimensional CSL is introduced by rotating the crystal lattice through an angle about a crystallographic axis and then two crystal lattices before and after the rotation are made to interpenetrate each other. A notation $\phi/[a_1, a_2, a_3, c]$ is used to describe the possible CSL relation with the rotation angle ϕ and the rotation axis $[a_1, a_2, a_3, c]$.

Figure 3 illustrates an $(11\bar{2}0)$ section through two interpenetrating crystal lattices generated by the rotation of an ice crystal lattice about $[11\bar{2}0]$ axis by an angle of 70.5° (i.e. 70.5°/$[11\bar{2}0]$).Atom positions marked by a squares represent coincidence-sites and then the value of Σ is 9. A unit cell of CSL is indicated by a dotted parallelepiped with the thickness of ice crystal unit length along $[11\bar{2}0]$.

Table 1. Possible CSL relations in ice crystals. *: CSL relation satisfying the bonding condition. Σ': Reciprocal density of coincidence-sites, when nearly perfect bonds are allowed. Type of snow polycrystal: *a* to *f* correspond to the types given in the caption of Fig. 1 and *g* the twelve-branched crystal.

$\phi/[a_1, a_2, a_3, c]$	Σ	Possible CSL boundaries	Type of snow polycrystal
*70.5°/$[11\bar{2}0]$	9	$\{30\bar{3}2\}/\{0001\}$ $\{30\bar{3}4\}/\{30\bar{3}4\}$	b, c, d, e
		$\{30\bar{3}8\}/\{30\bar{3}8\}$ $\{11\bar{2}0\}/\{11\bar{2}0\}$	
86.6°/$[11\bar{2}0]$	11	$\{10\bar{1}2\}/\{10\bar{1}2\}$	d
29.8°/$[11\bar{2}0]$	35	$\{20\bar{2}1\}/\{20\bar{2}1\}$	
55.9°/$[11\bar{2}0]$	36	$\{10\bar{1}1\}/\{10\bar{1}1\}$	d, f
*38.9°/$[11\bar{2}0]$	54	$\{30\bar{3}2\}/\{30\bar{3}2\}$ $\{30\bar{3}7\}/\{0001\}$	
78.5°/$[10\bar{1}0]$	10	$\{11\bar{2}4\}/\{11\bar{2}4\}$	f
62.9°/$[10\bar{1}0]$	11	$\{11\bar{2}2\}/\{11\bar{2}2\}$	f
*44.4°/$[10\bar{1}0]$	14	$\{11\bar{2}8\}/\{11\bar{2}8\}$	
		$\{11\bar{2}1\}/\{11\bar{2}6\}$ $\{10\bar{1}0\}/\{10\bar{1}0\}$	(glacier ice)[1]
23.1°/$[10\bar{1}0]$	25	$\{33\bar{6}2\}/\{33\bar{6}2\}$	
*60.0°/[0001]	2	{0001}/{0001}	a
*21.8°/[0001]	7	{0001}/{0001}	g
*27.8°/[0001]	13	{0001}/{0001}	g
*13.2°/ [0001]	19	{0001}/{0001}	
*17.9°/[0001]	31	{0001}/{0001}	
*30.6°/[0001]	97 ($\Sigma' = 14$)	{0001}/{0001}	g

[1]See Matsuda and Wakahama (1978).

Possible CSL relations with relatively low values of Σ in ice crystal lattice are listed in Table 1. When atoms in nearest neighboring positions are not bonded in fixed directions as the case of metallic bonds, only the fitting of atomic position between two mutually penetrating crystal lattices constitutes a possible CSL boundary with the low energy. Consequently, the values of Σ directly relate to the energy of CSL boundary. In case of the ice crystal, however, not only the value of Σ but also the fitting of bonding directions must be considered for the condition of low energy CSL boundary, because the hydrogen bonds are fixed to tetrahedral directions in an ice crystal lattice (Furukawa, 1976, 1982). Asterisks in Table 1 indicate the CSL relations which meet the criterion of the bond fitting. As a result of synthetic judgment, we concluded that the CSL relation of $70.5°/[11\bar{2}0]$ is probably the only one realized actually to form a low energy boundary.

3. Cubic Ice Nucleation Model at the Formation of Snow Polycrystals

It is known that there is a metastable cubic analogue of the stable hexagonal ice (I_h) structure (Wurtzite structure). The cubic ice (I_c) structure is called a diamond structure and differs only through the stacking sequence of oxygen atoms from the hexagonal structure. Consequently, the arrangement of oxygen atoms (or hydrogen bonds) along the {111} planes of cubic ice is identical with that along the {0001} planes of hexagonal ice.

Figure 4 schematically indicates an octahedral crystal form of cubic ice, which is surrounded by eight distinct {111} faces (Furukawa, 1982). Now, we observe that the {111} face of cubic ice can be connected to the {0001} face of hexagonal ice with no violation of immediate coordination requirements excepting the stacking

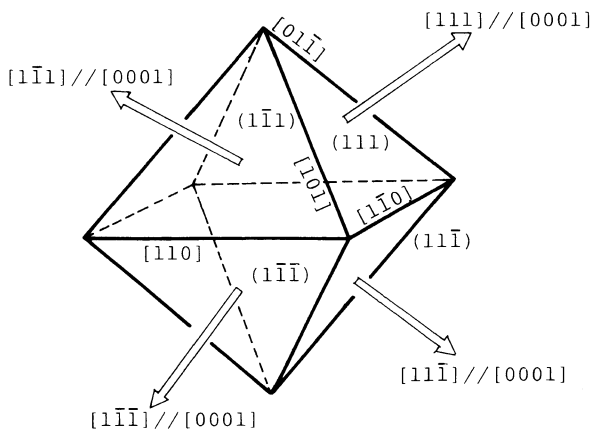

Fig. 4. Octahedral crystal form of metastable cubic ice; indicating the directions of successive growth of stable hexagonal ice.

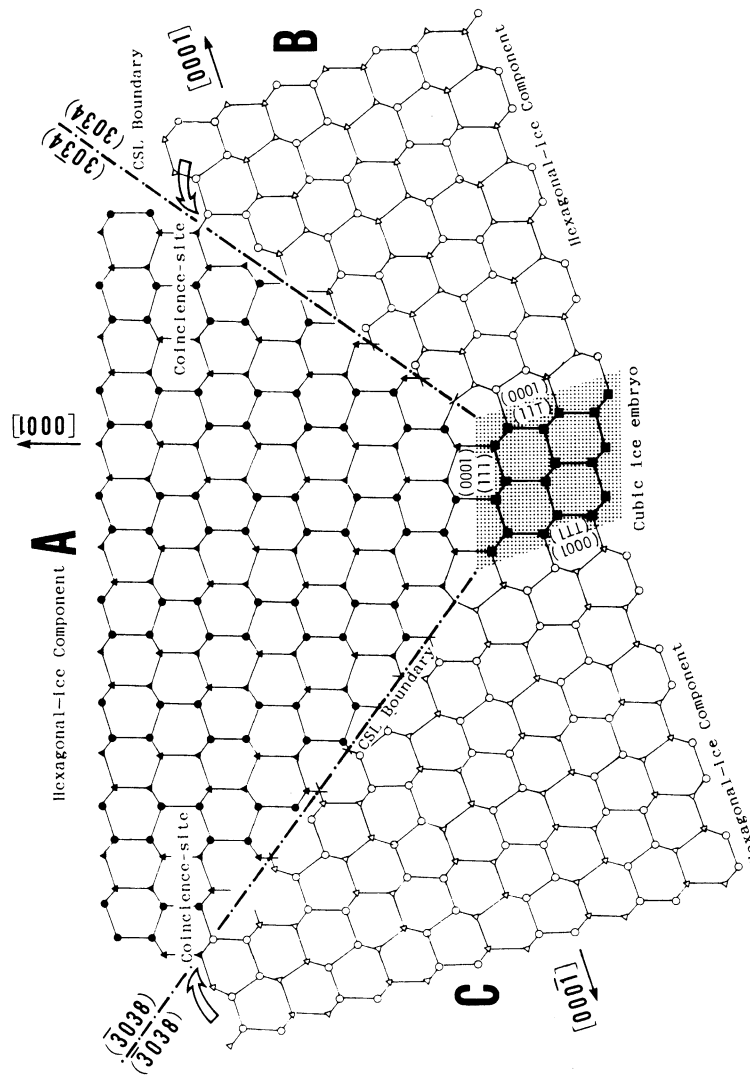

Fig. 5. Illustration of cubic ice embryo and structures of grain boundaries between neighboring hexagonal components, which have successively grown from the cubic embryo. Circles and triangles represent the oxygen atoms, and solid lines connecting them the hydogen bonds: projected along [11$\bar{2}$0].

fault at the composition plane and that the plane angle between each of {111} is 109.5° (namely, its supplementary angle is 70.5°). Let us consider that a metastable cubic ice embryo is initially formed and then converts to the stable hexagonal ice during the ice nucleation process in the supercooled cloud droplet. Figure 5 shows an illustrative case of a cubic embryo and hexagonal ice components extending from the cubic ice embryo. It is to be noted that the boundary structures between neighboring hexagonal components satisfy the CSL relation of 70.5°/[11$\bar{2}$0], which realize the lowest energy boundary in ice polycrystals. The polycrystalline initial-crystal (namely, frozen droplets) formed in this nucleation process grows subsequently into any type of snow polycrystals. Consequently, c-axes angles between each component of snow polycrystal should concentrate at 70° as an inevitable consequence.

The cubic ice nucleation model mentioned above has been watched with keen interest by many researchers ever since.

First, Takahashi (1982) and Takahashi and Kobayashi (1983) theoretically discussed the competition of a cubic ice embryo with that of a hexagonal one during ice nucleation from the supercooled water droplet on the basis of the concept of Ostwald's step rule. As a result, they concluded that the formation of the cubic ice embryo may be more probable rather than the formation of the hexagonal one at temperatures below –2°C.

On the other hand, a series of freezing experiments of supercooled water droplets were conducted by Uyeda and Kikuchi (1976b, 1980). They showed that the c-axes angles between each component of a polycrystalline frozen droplets are predominantly concentrated at 70°. Mizuno and Wakahama (1983) also studied the structures of frozen droplets on ice substrates using X-ray diffraction and obtained the similar result as one of Uyeda and Kikuchi. Recently, Mayer and Hallbrucker (1987) examined the water droplets rapidly quenched on a chilled substrate, using both X-ray diffraction and calorimetry (DSC). As a result, they showed that the cubic ice can be formed by the quenching of liquid water at $\leq$200 K and it transforms much more slowly to the stable hexagonal ice compared with the transformation of cubic ice formed by the vapor deposition. All of these experimental results are consistent with the cubic ice nucleation model.

Furthermore, as to evidence for the formation of cubic ice in the atmosphere, Whalley (1981) suggested that Scheiner's halo which occasionally occurs at 27.46° from the sun can be produced by light passing through octahedral cubic ice crystals as shown in Fig. 4.

4. Conclusions

Polycrystalline initial-crystals formed by freezing of the supercooled cloud droplets develop into either of two categories of snow polycrystals. The first category represents the case in which each component of an initial-crystal develops independently, its morphology depending on the conditions as the case with the

individual growth of snow single crystals. As a matter of course, snow polycrystals are constructed as the assemblages of single crystals in plate-like or prism-like shapes; that is, spatial dendrite, radiating dendrite, combination of bullets and so on.

The second category represents the case in which the initial-crystal grows in the direction along the grain boundary and its neighboring components interact each other. This directional growth is interpreted by such the mechanism as the CSL boundary including grain-boundary dislocations (GBDs) acts as the continuous source of growth steps on the ice surfaces (Furukawa and Kobayashi, 1978). A typical type of snow polycrystals in this category is a crossed-plates crystal, which grows by the action of GBDs on 70.5°/[11$\bar{2}$0] CSL boundary. The snow crystals of low temperature types (e.g. peculiar-shaped crystal), which are frequently observed in the polar regions (Kikuchi, 1970), are also included in this category. For the detailed explanation of this growth mechanism, see the other review papers (Furukawa, 1982; Kobayashi and Kuroda, 1987).

REFERENCES

Furukawa, Y. (1976), "On the structure of twin interfaces in ice crystals", J. Japan Assoc. Crystal Growth, **3**, 48–56.

Furukawa, Y. (1982), "Structures and formation mechanisms of snow polycrystals", J. Met. Soc. Jpn., **60**, 535–547.

Furukawa, Y. and Kobayashi, T. (1978), "On growth mechanism of polycrystalline snow crystals with a specific grain boundary", J. Crystal Growth, **45**, 57–65.

Kikuchi, K. (1970), "Peculiar shapes of solid precipitation observed at Syowa Station, Antarctica", J. Met. Soc. Jpn, **48**, 343–349.

Kobayashi, T. and Furukawa, Y. (1975), "On twelve-branched snow crystals", J. Crystal Growth, **28**, 21–28.

Kobayashi, T., Furukawa, Y., Takahashi, T., and Uyeda, H. (1976), "Cubic structure models at the junction in polycrystalline snow crystals", J. Crystal Growth, **35**, 262–268.

Lee, C. W. (1972), "On the crystallographic orientation of spatial branches in natural polycrystalline snow crystal", J. Met. Soc. Jpn., **50**, 171–180.

Matsuda, M. and Wakahama, G. (1978), "Crystallographic structure of polycrystalline ice", J. Glaciology, **21**, 607–620.

Mayer, E. and Hallbrucker, A. (1987), "Cubic ice from liquid water", Nature, **325**, 601–602.

Mizuno, Y. and Wakahama, G. (1983), "Structure and orientation of frozen droplets on ice substrate", J. Phys. Chem., **87**, 4161–4167.

Phmphley, P. H. (1976), "Special high angle boundaries", Grain boundary structure and properties, Academic Press, 139–200.

Takahashi, T. (1982), "On the role of cubic structure in ice nucleation", J. Crystal Growth, **64**, 441–449.

Takahashi, T. and Kobayashi, T. (1983), "The role of the cubic structure in freezing of a supercooled water droplet on an ice substrate", J. Crystal Growth, **64**, 593–603.

Uyeda, H. and Kikuchi, K. (1976a), "Remeasurement of axial angle between spatial branches of natural polycrystalline snow crystals", J. Fac. Sci., Hokkaido Univ., **VII5**, 21–28.

Uyeda, H. and Kikuchi, K. (1976b), "On the orientation of the principal axis of frozen droplets", J. Met. Soc. Jpn., **54**, 267–276.

Uyeda, H. and Kikuchi, K. (1980), "Measurements of the principal axis of frozen hemispheric water droplets", J. Met. Soc. Jpn., **58**, 52–58.

Whalley, E. (1981), "Scheiner's halo: Evidence for ice I_c in the atmosphere", Science, **211**, 389–390.